Chapter 2

DARK MATTER MODELS.

2.1 Introduction

Astronomers have spent many nights asleep to characterize those "unseen matter". Still now, they are searching for the ingredients that best suits for it. A few questions, like what is the kind of dark matter? What are the amount of the dark matter that the universe contains? How was the observed structure of the universe formed? How did the dark matter affect this? – puzzle those astronomers as well as those physicists who are trying to solve the "unseen mass" problem. There are mainly two expedients that one can foster in confronting with these challenges. One is, the most popular approach at present, a phenomenological approach where one can introduce a minimum number of new parameters (for example – a cosmological constant) to the standard model and try to obtain the best fitted model which can fit as many data as possible. The other one is a theoretical one in which one tries to construct a model which is most appealing from the logical point of view, based on the fundamental principles.

There are several candidates in the literature to present dark matter in the universe. We will now discuss some of them.

2.2 Dark Matter Models

2.2.1 Cold Dark Matter (CDM) model

Cold Dark Matter (CDM) [1, 2, 3] is an important candidate to describe dark matter and played an important role in galaxies formation scenario. With the word 'cold', we mean particles in this model move much slower than the speed of light. According to that model, if cold dark matter is the only candidate to form dark matter, then galaxies would form first and latter assemble them into clusters. In CDM model, structure has grown up hierarchically – small structures collapsed under their self-gravity and merged to form larger and more massive objects i.e. galaxy formed first then the clusters [4]. This is appreciated by the observations. In the history of the CDM model, in 1982, Peebles found evidences for a cold pressureless medium as the key player of structure formation of the universe. George Blumenthal, Sandra Faber, Joel Primack and Martin Rees accepted the role of CDM in galaxy formation[5]. As the matter is cold, there is no limit on the density of CDM particles in the galaxy halo. So, cold dark matter particles can adjust well into very low-mass galaxies. CDM will follow the following properties:

i. Being dark, dark matter does not interact, reflect or radiate energy in the form of electromagnetic spectrum. So, it would have to lack of interaction with the electromagnetic force.

ii. CDM particles would have to interact with any gravitational field through the gravitational interaction only.

iii. Weak interactions may be a property of some dark matter candidates, like neutrinos and neutrino-like particles. Other candidates, like axions, may not necessarily interact with the weak force.

The most recent researches indicate to a universe filled with a mixture of both cold dark matter and hot dark matter; the bulk of the dark matter is cold, but a very small fraction is hot (p.-124 of Ref.[6]). Elementary particle theory assumes several candidates like Weakly Interacting Massive Particles (WIMPs) [7, 8, 9, 10], Axions [11, 12], Massive Compact Halo Objects (MACHOs)[13] etc. for the particle that makes the CDM.

Some problems of CDM models :

Despite the successes of the CDM model to describe cosmological observations such as the large scale distribution of galaxies, the temperature variations in the cosmic microwave background radiation and the recent acceleration of the universe [14, 15, 16, 17] – recent observations on different types of galaxies have revealed that this model faces serious conflicts when trying to explain the galaxy formation at small scale [18]. Several discrepancies between the predictions of the particle cold dark matter paradigm and observations of galaxies and their clustering have raised. The large scale simulations of collissionless cold dark matter show that the density distribution in the inner region of DM halos obeys the power law $\rho \approx r^{\alpha}$ with $\alpha \approx -1$ [19]. This type of behavior is commonly known as cusp. But different observations, mainly on dwarf and LSB galaxies, showed that this is not the case rather they will follow $\rho \approx r^{0}$ [20, 21] in the inner region of DM halo. This discrepancy between observation and the prediction of CDM model for the case of density profile is known as cusp/core problem [22].

With the received data from a wide range of galaxies of different morphologies, Donato et al. (2009) [23] fit their rotational curves (RC) with the help of Burkert profile for the DM (Burkert 1995) [24]. Donato et al. found that

$$\lg(\mu_0/M_{\odot}pc^{-2}) = 2.15 \pm 0.2, \tag{2.1}$$

remains approximately constant where

$$\mu_0 = \rho_0 r_0, \tag{2.2}$$

ρ_0 is the central DM density and r_0 is the core radius. Kormendy & Freeman (2004); Spano et al. (2008) [25] are few well known names in that context. The galaxies, in the CDM model, have revolved through huge number of mergers and developed in different environments. So, the star formation and basic properties of the galaxies will expected to vary from galaxy to galaxy. Therefore, expounding both the constancy of μ_0 and the core in the central regions of galaxies seems very unlikely in this model [4].

According to CDM model, galaxies are formed by a hierarchical clustering process in which galaxies were came of by merging and accretion of numerous satellites of different sizes and masses. All of the accreted satellites may not be abolished by the ongoing process; as for example, the satellites of our own galaxy and of M31. CDM model foretold that a halo with the size of our galaxy should have about 50 dark matter satellites and their velocity should be more than 20 km/s with the mass $> 3\times 10^8 M_\odot$ within the radius of 570 kpc. This number of satellites is sufficiently higher than the approximately dozen satellites really observed around our galaxy. There should have approximately 300 satellites inside a 1.5 Mpc radius while only nearly 40 satellites are found in the Local Group. Therefore, a large fraction of the Local Group satellites has been missed in observations – that arise the dramatic discrepancy between observations and CDM model, regardless of the model parameters. This is known as "the missing satellites problem" [26].

Observations suggest that dwarf galaxies around the Milky Way and Andromeda galaxies are orbiting in thin planar structures. But, simulations foretell about the random distribution around their parent galaxies [27]. This is the well known "disk of satellites problem".

Looking at those problems, physicists are searching for alternative ones. Scalar Field Dark Matter (SFDM) model is a such one.

2.2.2 Scalar Field Dark Matter (SFDM) model

Physicists have suspected that the scalar field could be a dark matter candidate at galactic scales. The idea that a scalar field would be a dark matter candidates was firmly established by a paper of Cho and Keum [28]. The reasons behind this are –

i. Numerical simulations suggest that the critical mass for structure formation in the Universe with a potential energy of the form [29]

$$V(\Phi) = V_0[cosh(\lambda\sqrt{\kappa_0}\Phi) - 1], \tag{2.3}$$

is

$$M_{crit} \simeq 0.1\frac{m_{Pl}^2}{\sqrt{V_0\kappa_0}} = 2.5 \times 10^{13} M_{\odot}, \tag{2.4}$$

where

$$V_0 \simeq (3 \times 10^{-27} m_{Pl})^4, \tag{2.5}$$

λ is a free parameters of the model, $\kappa_0 = 8\pi G$ and $m_{Pl} \equiv G^{-1/2} \approx 10^{-5}g$ is the Planck mass. This is an astonishing result in the sense that using the same scalar field for analyzing the dark matter at relativistic scales, it will always collapse with a mass which corresponds to the halo of a real galaxy. Thus, this result foretells that SFDM model may be use to describe the galaxy formation.

ii. The behaviors of the scalar field and a dust fluid, like CDM, during the linear regime of cosmological fluctuations are similar. The density contrast in the SFDM model evolve in exactly the same form as we see in the CDM model. So, the large scale structure formation in the Universe for both models are same. The differences in their predictions on galaxy formation begin to appear in the non linear regime of structure formation [29].

iii. A scalar field object contains a flat central density profile, as seems to be the case in galaxies [29].

iv. A scalar field has no interaction with the rest of the matter and it can form a Bose condensate and thus could behave strictly as cold dark matter from the beginning [29].

Contribution of the luminous matter, gasses and scalar dark matter to the tangential velocity of spiral galaxies

Quintessence [30], a dynamical slow evolving spatially inhomogeneous scalar field, may be an explanation for dark matter and dark energy [31, 32]. Let us consider the standard static spherically symmetric line element describing the dark matter halo given by

$$ds^2 = -B(r)c^2dt^2 + A(r)dr^2 + r^2(d\theta^2 + \sin^2\theta d\phi^2), \tag{2.6}$$

where A and B are arbitrary functions of the coordinate r.

Consider, also, the scalar field action [33]

$$S = \int d^4x\sqrt{-g}[-\frac{R}{\kappa_0} + 2(\nabla\Phi)^2 - V(\Phi)], \tag{2.7}$$

where R is the scalar curvature, Φ is the scalar field, $\kappa_0 = 8\pi G$ and $V(\Phi) = \Lambda e^{-2\kappa_0\Phi}$. Therefore, Klein-Gordon and Einstein's equations can be obtained, respectively, as

[33]

$$\Phi^{;\mu}_{;\mu} - \frac{1}{4}\frac{dV}{d\Phi} = 0, \tag{2.8}$$

$$R_{\mu\nu} = \kappa_0[2\Phi_{,\mu}\Phi_{,\nu} + \frac{1}{2}g_{\mu\nu}V(\Phi)], \tag{2.9}$$

where $R_{\mu\nu}$ is the Ricci tensor and a semicolon stands for covariant derivative with respect to the background space-time; μ, ν = 0, 1, 2, 3. An exact solution for the system of Eqs.(2.8) and (2.9) can be taken as [33]

$$ds^2 = -f_0c^2(r^2+b^2\sin^2\theta)dt^2 + \frac{r^2+b^2\cos^2\theta}{f_0}(\frac{dr^2}{r^2+b^2}+d\theta^2) + \frac{r^2+b^2sin^2\theta}{f_0}d\phi^2. \tag{2.10}$$

With the assumptions that a galaxy is a virilized system and the space-time is due to the scalar field, the total circular velocity of a test particle can be expressed as [33]

$$v_{tg}^2 = v_L^2(f_0(r^2+b^2)+1), \tag{2.11}$$

where v_L is the circular velocity of the test particle due to the contribution of the luminous matter only. This velocity profile greatly coincides with the observed one and the contribution of luminous matter to the circular velocity ($v_L = v^2(R_{opt})\beta\frac{1.97x^{1.22}}{(x^2+0.78^2)^{1.43}}$ [33]) is a very convincing phenomenological model. In other word, this result firmly established the assumption that the scalar field could be a good viable alternative candidate to the dark matter in the halos of galaxies.

Considering individual contributions due to the luminous matter, the gas and the dark matter, the velocity along circular trajectories in the equatorial plane of the galaxy can be taken as [34]

$$v_{tg}^2 = v_L^2(1 + f_0(r^2 + b^2)) + v_{gas}^2, \tag{2.12}$$

with the parameters f_0 and b are to be chosen to adjust to the observed RC. With $v_L^2(r) = \frac{GM_L(r)}{r}$ ($M_L(r)$ is the total luminous mass at a distance r from the center of the galaxy), expression (2.12) simplifies to [34]

$$v_{tg}^2 = \frac{GM_L(r)}{r}(1 + f_0(r^2 + b^2)) + v_{gas}^2. \tag{2.13}$$

This individual contribution from luminous matter, gas and the scalar field to the velocity fits the observe RC of the galaxies with a quite good agreement (within 5% in all cases). In other words, the dark matter in the universe could be in the form of the scalar field. As a consequence, the question arises is that if the dark matter is in the form of the scalar field then how much the universe contains it ?

Measurement of the amount of dark matter

Observing the galaxy clusters and dynamical mass measurements in galaxies, it was found that the main components of the Universe are matter and vacuum energy and given by $\Omega_0 = \Omega_M + \Omega_\Lambda$ with $\Omega_M \sim 0.4$ [35]. Experiments on the Cosmic Background Radiation and measurements of the mass power spectrum propose that the acceptable value of Ω_0 for the Universe is $\Omega_0 = 1$. Therefore, $\Omega_\Lambda \sim 0.6$ which has the good agreement with observations of **Ia** supernovae [36, 37]. The matter component Ω_M is made of with baryons, neutrinos, etc. and dark matter. Considering the contribution of stars and dust, it was found that $\Omega_M = \Omega_b + \Omega_v + ... = 0.05 + \Omega_{DM}$ where Ω_{DM} represents the dark matter part of the matter contributions which has a value $\Omega_{DM} \sim 0.35$. Therefore, $\Omega_{DM} + \Omega_\Lambda \sim 0.95$ i.e. dark matter and dark energy form 95% of the whole matter in the Universe without any information about the nature of the dark matter Ω_{DM} or of the dark energy Ω_Λ.

Solution of a spherical symmetric and static line element describing the scalar dark matter halo and it's validity

If the dark matter is in the form of the scalar field then what would be the nature of the scalar potential ? To answer this question, let us consider the energy momentum tensor

$$T_{\mu\nu} = \Phi_{,\mu}\Phi_{,\nu} - \frac{1}{2}g_{\mu\nu}\Phi^{,\sigma}\Phi_{,\sigma} - g_{\mu\nu}V(\Phi), \tag{2.14}$$

where Φ and $V(\Phi)$ are the scalar field and the scalar potential, respectively. Then Klein-Gordon and Einstein equations are, respectively,

$$\Phi^{;\mu}_{;\mu} - \frac{dV}{d\Phi} = 0, \tag{2.15}$$

$$R_{\mu\nu} = \kappa_0[\Phi_{,\mu}\Phi_{,\nu} + g_{\mu\nu}V(\Phi)], \tag{2.16}$$

where $R_{\mu\nu}$ is the Ricci tensor, $\kappa_0 = 8\pi G$ and a semicolon stands for covariant derivative with respect to the background space-time; μ, $\nu = 0, 1, 2, 3$.

For particles in stable circular orbits, the tangential velocity can be obtained as [38]

$$(v_{tg})^2 = \frac{rB'}{2B}, \tag{2.17}$$

(where prime means derivative with respect to r). As the tangential velocity in the region far away from the centre of the galaxy to be constant, the above expression (2.17) yields $B = B_0 r^l$ where l is given by $l = 2(v_{tg}/c)^2$ and $B_0 > 0$ is an integration constant. As v_{tg}/c is nearly constant at a value 7×10^{-4} in the halo region, it is reasonable to take $l \sim 10^{-6}$ [39]. There after the metric (2.6) becomes

$$ds^2 = -B_0 r^l dt^2 + A(r)dr^2 + r^2 d\theta^2 + r^2 \sin^2\theta d\varphi^2. \tag{2.18}$$

Solution of Klein Gordon equation and Einstein equations with the help of the metric (2.18) are given by [40]

$$V(r) = -\frac{l}{\kappa_0(2-l)}\frac{1}{r^2}, \tag{2.19}$$

$$A(r) = \frac{4-l^2}{4+D(4-l^2)r^{-(l+2)}}, \tag{2.20}$$

where D be an integration constant. Thus, for a spherically symmetric metric with the flat rotational curve condition, the scalar potential varies as $V \propto \frac{1}{r^2}$. Observe that for the particular solution with $D = 0$ (if it possible) the stress tensor goes like $1/r^2$. Again, as $(\Phi_{,r})^2 \sim 1/r^2$ then $\Phi \sim \ln(r)$ indicating that the scalar potential $V \sim \exp(2\alpha\Phi)$. Such exponential scalar potential has been found very effective for the structure formation scenarios and also in quintessential scenarios. Despite the success of describing the flatness and matter density of the universe, this solution faces some unavoidable situations regarding the constants of integration D which we will discuss in the next few paragraphs.

Constraint on the arbitrary constant

A crucial condition that has to satisfy by any valid metric and so for the metric (2.6) is that $A(r) > 1$ which is also essential for signature protection of the metric. Now, for the sake of simplicity, if we choose $D = 0$, it will make the metric component $A < 1$. Thus to see the true picture of the model described above, it is necessary to proceed further with $D \neq 0$.

The density and pressure profiles in the rest frame of the fluid can be found as [41]

$$\begin{aligned}
\rho &= \frac{1}{8\pi}\frac{r^{-(4+l)}[D(l^3+l^2-4l-4)+l^2r^{2+l}]}{l^2-4},\\
p_r &= \frac{1}{8\pi}\frac{r^{-(4+l)}[D(l^3+l^2-4l-4)-l(4+l)r^{2+l}]}{l^2-4},\\
p_t &= \frac{1}{8\pi}\frac{r^{-(6+l)}[D(l^3+l^2-4l-4)+l^2r^{2+l}][(r^2-1)l-2(r^2+1)]}{4(l^2-4)}, \qquad (2.21)
\end{aligned}$$

where ρ, p_r and p_t are the energy density, radial pressure and transverse pressures, respectively. A non zero value of D is very essential to get rid off from repulsive gravity and also to determine the correct relativistic strengths between pressure and density.

For the value $D = 1$, for instance, in the distant halo region i.e. at $r \sim 100 - 300$ kpc and with $l \sim 10^{-6}$, the numerical values of the energy density to be $\rho \sim 10^{-9}$ and $p_r \sim 10^{-9}$ i.e. they are of the same order while $p_r + 2p_t \sim 10^{-11} \Rightarrow p_r + 2p_t \sim 10^{-2}\rho$ which reads that the density is nearly one hundred times larger than the total pressure. Similarly, for $D = 10^{-5}$, we find that $p_r + 2p_t \sim 10^3\rho$. Further decreasing the value of

D, but never exactly to zero, we can arrive at the conclusion that the total pressure dominates more and more over density reinforcing the non-Newtonian nature. For the survival of the Weak Energy Condition (WEC) and attractive nature of the gravity in the halo, we have to impose a limit on D.

The value $D = 10^{-7}$ corresponds to the extreme possible non-Newtonian halo in the scalar field model under consideration with $\omega = \frac{p_r+2p_t}{3\rho} = 3 \times 10^5$ (attractive gravity) (*Figure* 2.1.). For $D = 10^{-8}$, we have $\omega > 0$ up to $r = 200$ kpc (attractive gravity) and $\omega < -1$ beyond $r = 200$ kpc (repulsive gravity). This value of D representing a transition from attraction to repulsion (*Figure* 2.2.). At $D = 10^{-9}$, we have $\rho < 0$, $\omega < -1$ (repulsive gravity) (*Figure* 2.3.), which shares the same adversity that also follows from the choice $D = 0$. Thus, we have to maintain the condition $D \geq 10^{-7}$ in order to acquit from repulsive gravity. As $\rho > 0$, $\rho + p_r > 0$, $\rho + p_r + 2p_t > 0$ i.e. the standard energy conditions are satisfied everywhere with this choice of D, we can recover the non exotic nature of the halo matter. Therefore, we can anticipate the attractive gravity in the halo.

To assure this, one can follow the direction by Lynden-Bell; Katz and Bicak [42], and deduce that the total gravitational energy (E_G) is indeed negative i.e. $E_G = 4\pi \int_{r_1}^{r_2} [1 - A^{\frac{1}{2}}]\rho r^2 dr < 0$ as $\rho > 0$, $[1 - A^{\frac{1}{2}}] < 0$ and $r_2 > r_1$. As the scalar field model corresponding to $D = 10^{-7}$ is highly non-Newtonian ($p_r + 2p = 10^6\rho$), a purely Newtonian definition of mass, $M(r) = 4\pi \int \rho r^2 dr$ is not applicable. However, the dynamical mass in the first post Newtonian order becomes $M_{pN}(r) = 4\pi \int (\rho + p_r +$

$2p_t)r^2dr = 10^6M(r)$ which clarifies the non-Newtonian nature of the model in terms of masses.

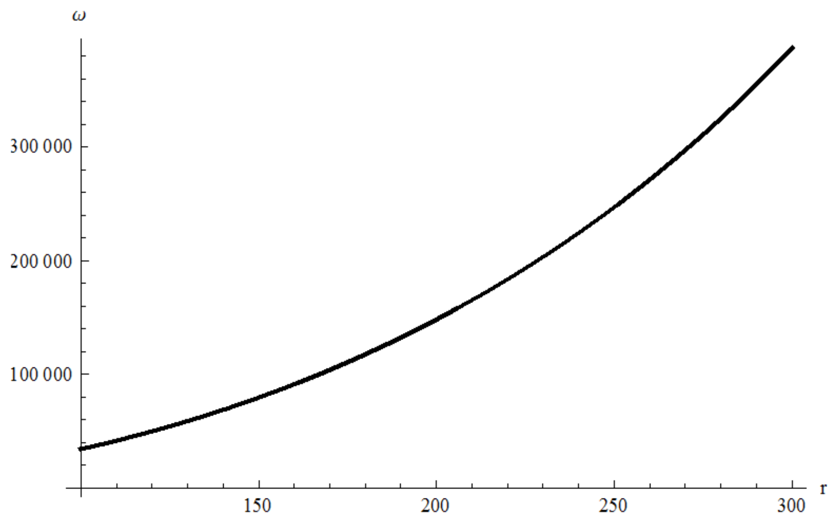

Figure 2.1. Plot of $\omega(r)$ vs r for $l = 10^{-6}$ and $D = 10^{-7}$. The distance r in galactic halo region is taken in the range $100 - 300$ kpcs. The non-Newtonian behavior of ω are evident.

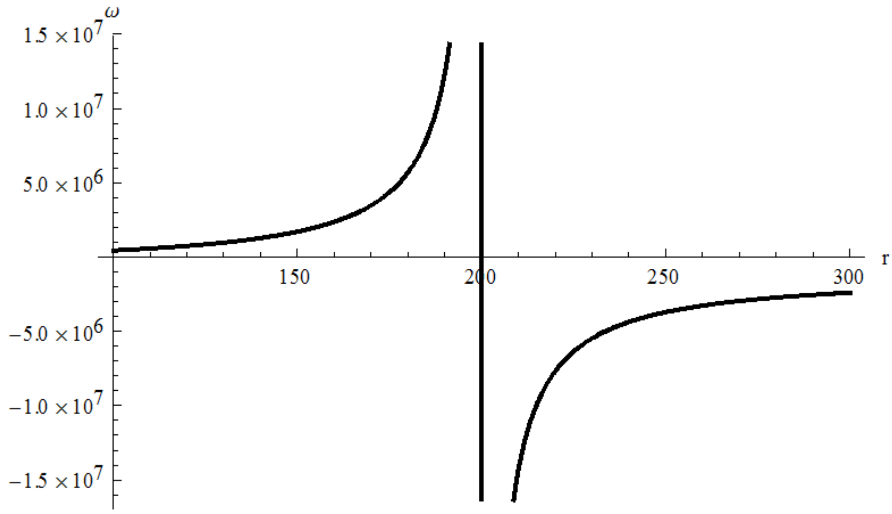

Figure 2.2. Plot of $\omega(r)$ vs r for $l = 10^{-6}$ and $D = 10^{-8}$. The distance r in galactic halo region is taken in the range $100 - 300$ kpcs. The figure displays the transition behavior of ω as discussed in the text.

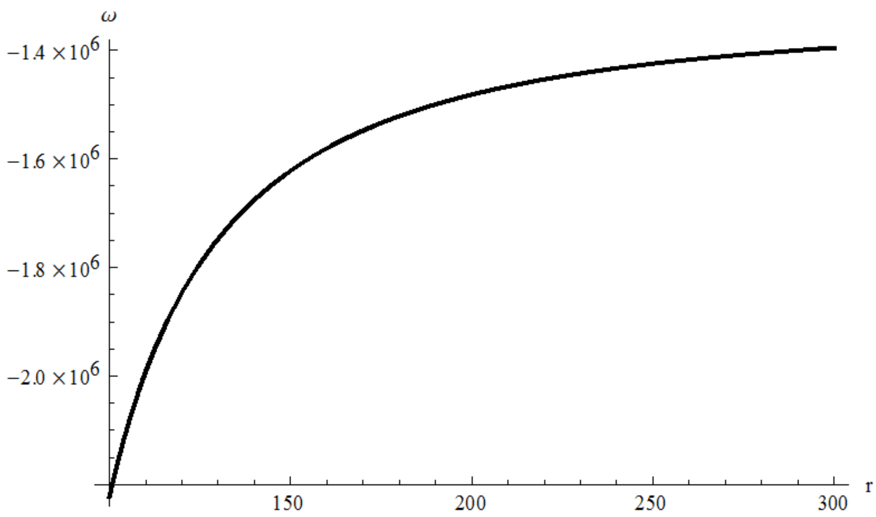

Figure 2.3. Plot of $\omega(r)$ vs r for $l = 10^{-6}$ and $D = 10^{-9}$. The distance r in galactic halo region is taken in the range 100−300 kpcs. The values of ω are negative indicating repulsive gravity.

Combine measurement of rotational curves and gravitational lensing: Introduction of pseudo profiles

Faber and Visser [43] have shown the way, how to measure the influence of the arbitrary constant 'D' on the equation of state and to find the contrast between the predictions and actual measurements. They proposed that in the first post-Newtonian approximation, the combined measurements of rotational curves and gravitational lensing permit us to decide not only about the mass and pressure profile of the galactic halo but also about the relation between energy density and pressure.

The static and approximately spherically symmetric gravitational field of a galaxy is represented by the space-time metric (Misner, Thorne & Wheeler, 1973),

$$ds^2 = -e^{2\Phi(r)}dt^2 + \frac{1}{1-\frac{2m(r)}{r}}dr^2 + r^2 d\theta^2 + r^2 \sin^2\theta d\varphi^2, \quad (2.22)$$

which is completely determined by the two metric functions $\Phi(r)$ and $m(r)$. Remember that one can not directly measure the metric functions but indirectly measures gravitational potentials and masses from rotation curve and lensing observations. The most general static and spherically symmetric stress-energy tensor along with the Einstein field equations give [43]

$$8\pi\rho = \frac{2m'(r)}{r^2}, \quad (2.23)$$

$$8\pi p_r(r) = -\frac{2}{r^2}[\frac{m(r)}{r} - r\Phi'(r)(1-\frac{2m(r)}{r})], \quad (2.24)$$

$$8\pi p_t(r) = -\frac{1}{r^3}[rm'(r) - m(r)][1 + r\Phi'(r)] + (1-\frac{2m(r)}{r})[\frac{\Phi'(r)}{r} + \Phi'(r)^2 + \Phi''(r)]. \quad (2.25)$$

Eq.(2.23) unveils the physical interpretation of $m(r)$ as the total mass-density within a sphere of radius r. One can recover standard Newtonian physics as the limit of general relativity where (Misner et al. 1973) :

i. the gravitational field is weak ($2m/r \ll 1$ or $2\Phi \ll 1$),

ii. the speed of the probe particles (v) involved are slow compared to the speed of light (c) i.e. $v^2/c^2 \ll 1$,

iii. the pressures and matter fluxes are small compared to the mass-energy density.

The mass $m_{RC}(r)$ which is inferred by the rotational curve measurements can be obtained as [43]

$$m_{RC}(r) = r^2 \Phi'_{RC}(r) \approx 4\pi \int (\rho + p_r + 2p_t) r^2 dr. \tag{2.26}$$

Therefore, in general, $m_{RC}(r) \neq m(r)$.

In general, the potentials obtained from rotation curve and lensing observations, Φ_{RC} and Φ_{lens} respectively, are not same [43] :

$$\Phi_{RC}(r) = \Phi(r), \tag{2.27}$$

and by definition

$$\Phi_{lens}(r) = \frac{\Phi(r)}{2} + \frac{1}{2} \int \frac{m(r)}{r^2} dr. \tag{2.28}$$

But, it is only in the Newtonian limit for which the condition (iii) holds, we get $\Phi_{RC} = \Phi_{lens}(r) = \Phi_N$.

With the Newtonian assumptions, the mass and the potential are related by a field equation of the form $\nabla^2(\Phi) \approx 4\pi\rho$. With these potentials, the rotational curve mass(m_{RC}) and lensing mass(m_{lens}) are define by [43]

$$m_{RC}(r) = r^2\Phi^{'}(r), \tag{2.29}$$

$$m_{lens}(r) = \frac{r^2\Phi^{'}(r)}{2} + \frac{m(r)}{2}, \tag{2.30}$$

which are equivalent to the potentials (2.27) and (2.28). Furthermore, the dimensionless quantity and the equation of state parameter is given by [43]

$$\omega(r) = \frac{p_r(r) + 2p_t(r)}{3\rho(r)} \approx \frac{2}{3}\frac{m^{'}_{RC}(r) - m^{'}_{lens}(r)}{2m^{'}_{lens}(r) - m^{'}_{RC}(r)}, \tag{2.31}$$

is an effective tool to measure the equation of state.

Thus, we see that rotational curve measurements provide a pseudo-mass profile $m_{RC}(r)$ while another pseudo-mass profile with different physical interpretation, $m_{lens}(r)$, is produced by gravitational lensing observations. A combination of this two pseudo-masses helps one to find the density and pressure profiles in the lensing galaxy via [43]

$$\rho(r) = \frac{1}{4\pi r^2}[2m^{'}_{lens}(r) - m^{'}_{RC}(r)], \tag{2.32}$$

$$p_r(r) + 2p_t(r) \approx \frac{2c^2}{4\pi r^2}[m^{'}_{RC}(r) - m^{'}_{lens}(r)] \tag{2.33}$$

(the factor c^2 is introduced in the formulae to make it suitable for SI unit).

Impact of the arbitrary constant

Now, we are eager to compute the impact of small non-zero values of 'D' on the analytic pseudo profiles. If the pseudo quantities that are observable from the combined measurement (i.e. that are on the right hand side of Eqs.(2.31)−(2.33)) agree with the analytic pseudo profiles coming from a known metric functions, the solution would be physically substantiated. Otherwise, it would be treated as non-viable.

From the metrics (2.6) and (2.22), we have

$$\Phi_{RC}(r) = \Phi(r) = \lg(B_0 r^l).$$

Therefore, the gravitational potential, rotational curve mass and gravitational lensing mass in Matos et al. solution [40], are given by

$$\Phi_{lens}(r) = \frac{1}{4}[Log[B_0] + lLog[r] + \frac{(-2+l)Dr^{-2-l} + l^2 Log[r]}{(l^2-4)}],$$

$$\begin{aligned} m_{RC}(r) &= \frac{lr}{2} \approx 10^{-6} r, \\ m_{lens}(r) &= \frac{r^{-1-l}[-(l^2-4)D + l(l^2+l-4)r^{2+l}]}{4(l^2-4)} \\ &\approx \frac{l(l^2+l-4)r}{4(l^2-4)} \approx 10^{-6} r. \end{aligned}$$

From Eq.(2.31),

$$\omega(r) \approx \frac{l(l^2-l-4)r^{2+l} - D(l^3+l^2-4l-4)}{3[D(l^3+l^2-4l-4) + l^2 r^{2+l}]}, \tag{2.34}$$

which within the range $r \sim (100-300)$ kpc and with $D = 10^{-7}$, yield $\omega \approx 3 \times 10^5$. If we put directly $D = 0$ in Eq.(2.34), we have $\omega < -1$, conveying a completely wrong physical interpretation about the halo. Therefore, we should have to maintain $D \geq 10^{-7}$ to avoid some unavoidable situations like $\omega < -1$. It is obvious that the lowest limit on D is quite small and nearly set to zero, although not, the price for setting it to zero is that one would see a completely wrong picture of the halo. Consequently, the solution of the metric (2.18) given by Eq.(2.20) would be a physically viable one on the restriction $D \geq 10^{-7}$.

References

[1] D. N. Spergel et al. (WMAP), Astrophys. J. Suppl. **170**, 377 (2007).

[2] M. Tegmark et al. (SDSS), Phys. Rev. D**74**, 123507 (2006).

[3] A. G. Riess et al., Astrophys. J. **659**, 98 (2007).

[4] Victor H. Robles and T. Matos, MNRAS, **422**, 282-289 (2012).

[5] Blumenthal, G., Faber, S. M., Primack, J. R., Rees, M; J. 1984, Nature, **311**, 517.

[6] Debasish Majumdar, Dark Matter - An Introduction, CRC Press (2014).

[7] G. Steigman and M.S. Turner, Nucl. Phys. B **253**, 375 (1985).

[8] G. Jungman, M. Kamionkowski and K. Griest, Phys. Rept. **267**, 195 (1996).

[9] L. Bergstrom, Rept. Prog. Phys. **63**, 793 (2000).

[10] G. Bertone, D. Hooper and J. Silk, Phys. Rept. **405**, 279 (2005).

[11] S. Weinberg, A new light boson?, Phys. Rev. Lett., **40**, 223–226 (1978).

[12] F. Wilczek. Problem of strong p and t invariance in the presence of instantons, Phys. Rev. Lett., **40**, 279–282 (1978).

[13] S. Banerjee, A. Bhattacharyya, S.K. Ghosh, S. Raha, B. Sinha and H. Toki, MNRAS **340**, 284 (2003).

[14] Coles P., Nature, **433**, 248-56 (2005).

[15] Lahav O., Liddle A.R., arXiv:1002:3488v1 (2010).

[16] Peebles P.J.E., Lyman A.P. Jr., Bruce R.P, Finding the Big Bang,

Cambridge University Press, 2009.

[17] Guo, Q. et al., MNRAS, **413**, 101 (2011).

[18] Friedmann D. E., J.Cosmol., **13** (2011).

[19]Navarro J.F. et al., MNRAS, **402**, 21 (2010).

[20] Wilkinson M.I., Kleyna J.T., Evans N.W. et al., ApJ, **611**, L21 (2004).

[21] Walker M.G., Penarrubia J., ApJ, **742**, 20 (2011).

[22] de Blok W.J.G., 2010, Adv. Astron., Article ID 789293 (2010).

[23] Donato et al., MNRAS, **397**, 1169 (2009).

[24] Burkert A., ApJ, **447**, L25 (1995).

[25] Spano M. et al., MNRAS, **383**, 297 (2008).

[26] Anatoly Klypin et al., ApJ, **522,** 82 (1999).

[27] Marcel Pawlowski et al., MNRAS (2014), arXiv:1406.1799v1 [astro-ph.GA], 6 Jun 2014.

[28] Y. M. Cho and Y. Y. Keum, Class. Quantum Grav., **15,** 907-921 (1998).

[29] A. Bernal, T. Matos and D. Nunez, arXiv:astro-ph/0303455**v3,** 18 Feb (2008).

[30] T. Matos and Urena Lopez, Class.Quant.Grav.**17**, L75-L81 (2000).

[31] R. R. Caldwell, Rahul Dave and Paul J. Steinhardt, Phys. Rev. Lett. **80** (1998).

[32] Ivaylo Zlatev, Limin Wangand Paul J. Steinhardt, Phys. Rev. Lett.

82, 896 (1998).

[33] T. Matos, and F. S. Guzman, Annalen Phys. **9,** S1-S133 (2000).

[34] F. S. Guzman, Tonatiuh Matos, Rev.Mex.Astron.Astrofis. **37,** 63-72 (2001).

[35] T. Matos, F. S. Guzman, L. A. Urena-Lopez, Class.Quant.Grav. **17,** 1707-1712 (2000).

[36] Perlmutter et al. ApJ **517**, 565 (1999).

[37] A. G. Riess et al., Astron. J. **116,** 1009-1038 (1998).

[38] Chandrasekhar, S. Mathematical theory of black holes, Oxford Science Publications (1983).

[39] A. Boriello and P. Salucci, Mon. Not. R. Astron. Soc. **323**, 285 (2001).

[40] T. Matos, F. S. Guzman and D. Nunez, Phys.Rev. D **62**, 061301 (2000).

[41] Nandi et al. Phys. Rev. D **80,** 047301 (2009).

[42] D. Lynden-Bell, J. Katz and J.Bicak, Phys. Rev. **D 75**, 024040 (2007).

[43] T. Faber and M. Visser, Mon. Not. R. Astron. Soc. **372**, 136 (2006).